

## A Contiguous Stretch of Methionine Residues Mediates the Energy-Dependent Internalization Mechanism of a Cell-Penetrating Peptide

Youngsoo Kim, Antonietta Lillo, Jason A. Moss, and Kim D. Janda\*

*The Skaggs Institute for Chemical Biology and Departments of Chemistry and Immunology,  
The Scripps Research Institute, 10550 North Torrey Pines Road, La Jolla, California 92037*

Received May 18, 2005

**Abstract:** Recently we characterized an unusual switch in the internalization mechanism of the monomeric and dimeric forms of the cell-penetrating peptide RDLWEMMMVSLACQY. Here, we observed both energy-dependent and energy-independent modes of peptide uptake by the target B-lymphocytes WI-L2-729HF2, suggesting that higher-order structure might modulate the action of this novel cell-penetrating peptide. In the present work, we propose a possible internalization mechanism for the dimeric peptide which involves an initial interaction with the cell membrane, followed by an energy-dependent internalization process which requires the contiguous Met(6–8) sequence.

**Keywords:** Cell-penetrating peptide; CPP; drug delivery; peptide; energy-dependent mechanism

### Introduction

The discovery and design of various cell-penetrating peptides (CPPs) has revolutionized intracellular drug delivery.<sup>1–3</sup> In the past decade, many potential drug delivery vectors have been studied based on CPPs derived from naturally occurring protein transduction domains such as Tat (from HIV-1) and penetratin (from *Antennapedia*).<sup>4–6</sup> Unique intracellular localizing regions have also been reported,

spurring the development of regioselective drug delivery vectors and the elucidation of general rules for cellular uptake mechanisms of CPPs.<sup>4–6</sup> In spite of this extensive work, the membrane translocation mechanisms of most CPPs remain to be unequivocally solved. The mechanism of transduction for most CPPs was assumed to involve passive diffusion through the plasma membrane in a receptor-independent manner that was not influenced by temperature, nor negatively affected by ATP depletion and secondary structure alteration.<sup>6–15</sup> However, this internalization mechanism has recently been questioned since new data has emerged

\* Corresponding author. Mailing address: Department of Chemistry, The Scripps Research Institute and the Skaggs Institute for Chemical Biology, 10550 N. Torrey Pines Rd., La Jolla, CA 92037. Tel: +1-858-784-2515. Fax: +1-858-784-2590. E-mail: kdjanda@scripps.edu.

- (1) Fischer, P. M.; Krausz, E.; Lane, D. P. Cellular delivery of impermeable effector molecules in the form of conjugates with peptides capable of mediating membrane translocation. *Bioconjugate Chem.* **2001**, *12* (6), 825–841.
- (2) Wright, L. R.; Rothbard, J. B.; Wender, P. A. Guanidinium rich peptide transporters and drug delivery. *Curr. Protein Pept. Sci.* **2003**, *4* (2), 105–124.
- (3) Joliot, A.; Prochiantz, A. Transduction peptides: from technology to physiology. *Nature Cell Biol.* **2004**, *6* (3), 189–196.
- (4) Green, M.; Loewenstein, P. M. Autonomous functional domains of chemically synthesized human immunodeficiency virus tat trans-activator protein. *Cell* **1988**, *55* (6), 1179.

- (5) Frankel, A. D.; Pabo, C. O. Cellular uptake of the tat protein from human immunodeficiency virus. *Cell* **1988**, *55* (6), 1189.
- (6) Derossi, D.; Joliot, A. H.; Chassaing, G.; Prochiantz, A. The 3rd Helix of the *Antennapedia* Homeodomain Translocates through Biological-Membranes. *J. Biol. Chem.* **1994**, *269* (14), 10444–10450.
- (7) Richard, J. P.; Melikov, K.; Vives, E.; Ramos, C.; Verbeure, B.; Gait, M. J.; Chernomordik, L. V.; Lebleu, B. Cell-penetrating peptides—A reevaluation of the mechanism of cellular uptake. *J. Biol. Chem.* **2003**, *278* (1), 585–590.
- (8) Suzuki, T.; Futaki, S.; Niwa, M.; Tanaka, S.; Ueda, K.; Sugiura, Y. Possible existence of common internalization mechanisms among arginine-rich peptides. *J. Biol. Chem.* **2002**, *277* (4), 2437–2443.

detailling receptor-, energy-, temperature-, and lipid-dependent cellular uptake mechanisms as observed with the TAT peptide.<sup>16–20</sup>

We recently reported on a CPP (RDLWEMMMVSL-ACQY) whose membrane translocation mechanism is controlled by a dimerization-dependent switch between energy-dependent and -independent fashions.<sup>21,22</sup> Confocal fluorescence microscopy revealed that both monomeric and homodimeric derivatives of this sequence were efficiently internalized into the target B-lymphocyte WI-L2-729HF2 cells, albeit

through different mechanisms. While internalization of the monomeric peptide is ATP-independent, suggesting passive diffusion across the cell membrane, internalization of the symmetrical dimer was virtually abolished by pretreating the target cells with the cytochrome oxidase inhibitor NaN<sub>3</sub>. To gain a more detailed insight into the membrane translocation mechanism of this sequence, we prepared a variety of analogues of the native sequence and studied their membrane translocation properties as well as solution-phase conformation.

## Experimental Section

**General Peptide Synthesis.** All peptides were prepared by stepwise solid-phase peptide synthesis (SPPS) using in situ neutralization protocols for Boc chemistry as previously described. All Boc amino acids were obtained from Senn Chemicals (Dielsdorf, Switzerland). *p*-Methylbenzhydrylamine (MBHA) resin was prepared by Advanced Chemtech on a custom synthesis at a loading of 0.64 mmol of NH<sub>2</sub>/g (100–200 mesh). Side-chain protections were as follows: Ser, Thr (Bzl), Asp, Glu (OcHex); W (formyl); Met (sulfoxide); Cys (MeBzl); Tyr (2-BrZ); Lys (Alloc); all other amino acids were incorporated without side-chain protection. Trifluoroacetic acid (Biograde) was from Halocarbon (River Edge, NJ); *N,N*-dimethylformamide (BioAnalyzed) was from J. T. Baker (St. Louis, MO); 7.5 M ammonium acetate solution was from Sigma (St. Louis, MO); *N,N*-diisopropylethylamine, fluorescein isothiocyanate, isomer 1, 90% (FITC), piperidine, and Pd(PPh<sub>3</sub>)<sub>4</sub> were from Aldrich (Milwaukee, WI); and anhydrous hydrogen fluoride (UHP) was from Matheson Gas (Cucamonga, CA). HF cleavage was performed in a type II vacuum-driven HF apparatus from Peptide Institute (Minoh, Osaka, Japan). All other reagents, solvents, and chemicals were of the highest purity commercially available and used as received. RP-HPLC was performed using binary gradients of solvents A and B, where A is 0.1% TFA in water and B is 0.09% TFA in acetonitrile. Analytical RP-HPLC was performed using a Vydac 218TP5415 column at a flow rate of 1 mL/min, with detection at 214 nm during a linear gradient of 20–80% B over 30 min. Preparative RP-HPLC was performed using a Vydac 218TP101522 column at a flow rate of 10 mL/min, with detection at 220 nm during a linear gradient of 35–55% B over 30 min. In all cases, fractions were analyzed off-line using an ABI/Sciex 150EX single quadrupole mass spectrometer and judged for purity after a consistent summing of 20 scans in multichannel analysis (MCA) mode, using the [M + 2]<sup>2+</sup> charged species. For preparative purification purposes, fractions that contained no single [M + 2]<sup>2+</sup> charged species which accounted for more than 10% of the total ion intensity were designated “pure” and pooled; the homogeneity of this pool was verified by analytical RP-HPLC and was >96%.

**Reduced Methionine Monomer (1a) and Dimer (1b).** The sequence NH<sub>2</sub>–RDLWEMMMVSLACQYK(Ahx-FITC)–CONH<sub>2</sub> was prepared by stepwise SPPS using methods essentially as described, although couplings were

- (9) Futaki, S.; Suzuki, T.; Ohashi, W.; Yagami, T.; Tanaka, S.; Ueda, K.; Sugiura, Y. Arginine-rich peptides—An abundant source of membrane-permeable peptides having potential as carriers for intracellular protein delivery. *J. Biol. Chem.* **2001**, *276* (8), 5836–5840.
- (10) Mitchell, A. From duckweed to DNA and from repair to remodelling. *Nat. Rev. Mol. Cell Biol.* **2000**, *1* (1), 7–7.
- (11) Wender, P. A.; Mitchell, D. J.; Pattabiraman, K.; Pelkey, E. T.; Steinman, L.; Rothbard, J. B. The design, synthesis, and evaluation of molecules that enable or enhance cellular uptake: Peptoid molecular transporters. *Proc. Natl. Acad. Sci. U.S.A.* **2000**, *97* (24), 13003–13008.
- (12) Vives, E.; Brodin, P.; Lebleu, B. A truncated HIV-1 Tat protein basic domain rapidly translocates through the plasma membrane and accumulates in the cell nucleus. *J. Biol. Chem.* **1997**, *272* (25), 16010–16017.
- (13) Mitchell, D. J.; Kim, D. T.; Steinman, L.; Fathman, C. G.; Rothbard, J. B. Polyarginine enters cells more efficiently than other polycationic homopolymers. *J. Pept. Res.* **2000**, *56* (5), 318–325.
- (14) Futaki, S. Arginine-rich peptides: potential for intracellular delivery of macromolecules and the mystery of the translocation mechanisms. *Int. J. Pharm.* **2002**, *245* (1–2), 1–7.
- (15) Wender, P. A.; Rothbard, J. B.; Jessop, T. C.; Kreider, E. L.; Wyllie, B. L. Oligocarbamate Molecular Transporters: Design Synthesis, and Biological Evaluation of a New Class of Transporters for Drug Delivery. *J. Am. Chem. Soc.* **2002**, *124*, 13382–13383.
- (16) Richard, J. P.; Melikov, K.; Brooks, H.; Prevot, P.; Lebleu, B.; Chernomordik, L. V. Cellular uptake of unconjugated TAT peptide involves clathrin-dependent endocytosis and heparan sulfate receptors. *J. Biol. Chem.* **2005**, *280* (15), 15300–15306.
- (17) Snyder, E. L.; Dowdy, S. F. Cell penetrating peptides in drug delivery. *Pharm. Res.* **2004**, *21* (3), 389–393.
- (18) Wadia, J. S.; Stan, R. V.; Dowdy, S. F. Transducible TAT-HA fusogenic peptide enhances escape of TAT-fusion proteins after lipid raft macropinocytosis. *Nat. Med.* **2004**, *10* (3), 310–315.
- (19) Vives, E.; Richard, J. P.; Rispal, C.; Lebleu, B. TAT peptide internalization: Seeking the mechanism of entry. *Curr. Protein Pept. Sci.* **2003**, *4* (2), 125–132.
- (20) Silhol, M.; Tyagi, M.; Giacca, M.; Lebleu, B.; Vives, E. Different mechanisms for cellular internalization of the HIV-1 Tat-derived cell penetrating peptide and recombinant proteins fused to Tat. *Eur. J. Biochem.* **2002**, *269* (2), 494–501.
- (21) Gao, C. S.; Mao, S. L.; Ditzel, H. J.; Farnaes, L.; Wirsching, P.; Lerner, R. A.; Janda, K. D. A cell-penetrating peptide from a novel pVII-pIX phage-displayed random peptide library. *Bioorg. Med. Chem.* **2002**, *10* (12), 4057–4065.
- (22) Moss, J. A.; Lillo, A.; Kim, Y. S.; Gao, C. S.; Ditzel, H.; Janda, K. D. A dimerization “switch” in the internalization mechanism of a cell-penetrating peptide. *J. Am. Chem. Soc.* **2005**, *127* (2), 538–539.

performed in DMSO/DMF (1:4, v/v), as we found that the inclusion of DMSO in the coupling cocktail greatly enhanced the purity of the final product. Although this undoubtedly led to some degree of oxidation of the Cys-13 residue *p*-methylbenzyl thioether during chain assembly, this predictable side reaction was reversed during the final side-chain-deprotection step. At the conclusion of chain assembly, the N-terminus was protected with Z-OSu, after which the Lys-16 Alloc side-chain protection was removed by overnight treatment with  $Pd(PPh_3)_4$  (0.2 equiv) and *N,N*-dimethylbarbituric acid (10 equiv) in 1:1  $CH_2Cl_2$ /DMF with orbital shaking under dark. The completeness of this deprotection step was verified by small scale (20 mg) HF cleavage followed by ESI analysis of the crude product. Boc- $\epsilon$ -aminohexanoic acid (Ahx) was then coupled to the newly unmasked Lys side chain, followed by Boc deprotection and FITC coupling. FITC (2 equiv) coupling was performed with *N,N*-diisopropylethylamine (1 equiv) in DMF for 2 h. The resin was then washed successively with DMF and  $CH_2Cl_2$ , dried in *vacuo* overnight, and global side-chain deprotection/cleavage was performed using the low–high HF method as previously described.<sup>23</sup> It should be mentioned that we found that quantitative deformylation required the use of 5% *p*-thiocresol, 5% *p*-cresol in 3:1 HF/DMS for 2 h, and that the purity of the final product was greatly enhanced if the resin was washed with  $CH_2Cl_2$  between the low and high cleavage steps. Following evaporation of HF after the high cleavage step, the crude peptide was triturated from ice-cold, peroxide-free diethyl ether, solubilized in 25% solvent B (vide supra), diluted with water, and lyophilized. The crude peptide was purified by preparative RP-HPLC and oxidized to yield the symmetrical dimer. For this reaction, a saturated solution of the peptide in 2:1 DMSO/7.5 M ammonium acetate solution was prepared and stirred in a closed vessel at 37 °C. Oxidation was complete after 24 h, after which this solution was diluted 2-fold and purified by semipreparative RP-HPLC with detection at 220 nm.

#### Oxidized Methionine Monomer (2a) and Dimer (2b).

Methionine sulfoxide mutants,  $NH_2$ –RDLWEM(O)M(O)M–O–VSLACQYK(Ahx–FITC)–CONH<sub>2</sub>, were prepared and dimerized in the same manner as **1a** and **1b**. However, methionine residues were left oxidized using the high HF protocol after deformylation of the tryptophan indole protection on the resin-bound peptide using 20% piperidine/DMF with orbital shaking for 2 h.

**Norleucine-Methionine (Nle6–8) Monomer (3a) and Dimer (3b).** Nle(6–8) substituted mutants,  $NH_2$ –RDLWE–NleNleNle–VSLACQYK(Ahx–FITC)–CONH<sub>2</sub>, were also prepared and dimerized in the same manner as **1a** and **1b**. However, the high HF protocol and the tryptophan deformylation were performed as in the case of the oxidized methionine monomer and dimer, **2a** and **2b**, respectively.

(23) Tam, J. P.; Heath, W. F.; Merrifield, R. B.  $S_{N}2$  Deprotection of Synthetic Peptides with a Low Concentration of HF in Dimethyl Sulfide: Evidence and Application in Peptide Synthesis. *J. Am. Chem. Soc.* **1983**, *105*, 6442–6455.

**Cell Line.** B-Lymphocyte WI-L2-729HF2 cells (American Type Culture Collection CRL-8062) were grown in RPMI 1640 medium supplemented with 10% fetal calf serum (FCS) in 6.5% CO<sub>2</sub> at 37 °C.

**Slide Preparation and Confocal Microscopy.** Fifty milliliters of WI-L2-729HF2 cell culture in modified RPMI 1640 medium with 10% FCS was grown at 37 °C, in a 7% CO<sub>2</sub> atmosphere, to exponential phase (~104 cells/mL). The cells were then centrifuged at 2000 rpm for 2 min, resuspended in 60 mL of fresh medium, and incubated for an additional 2 h at 37 °C in a 7% CO<sub>2</sub> atmosphere. The culture was then split into six aliquots of 10 mL. An aqueous solution of NaN<sub>3</sub> (final concentration = 0.03%) was added to half of the aliquots, and the incubation continued for an additional 30 min. The synthetic peptides **1a**, **1b**, **2a**, **2b**, **3a**, and **3b** (final concentration of each 1.97  $\mu$ M) were each added to one of the cell suspensions lacking sodium azide and one of the untreated cell suspensions, for a total of six samples. The cultures were incubated at 37 °C for 2 h in a 7% CO<sub>2</sub> atmosphere. The cells were washed 10 times in RPMI medium containing 10% FCS by multiple cycles of centrifugation (2000 rpm, 2 min) and resuspension in medium. The cells were resuspended in PBS containing 0.05% trypsin and 0.5 mM EDTA, incubated at 37 °C for 5 min, and then washed four times in RPMI 1640 medium containing 10% FCS. After the last centrifugation each cell pellet was resuspended in 100  $\mu$ L of PBS. Next, 30–60  $\mu$ L portions of these cell suspensions were spun onto microscope slides by cytocentrifugation (cytocentrifuge model MN 21211A from Minarik Electronics, Los Angeles, CA) for 3 min at 50 rpm. The cells were then fixed and permeabilized by addition of one drop of 95% ethanol in water and 5 min incubation at room temperature. Upon five washes with PBS, the slides were blocked with 500  $\mu$ L of 10% BSA in PBS for 30 min at room temperature and stained with propidium iodide (final concentration 10  $\mu$ g/mL, 5 min incubation). After 10 washes in PBS and addition of 25  $\mu$ L of antifade reagent (Slow-Fade Light Antifade Kit, Molecular Probes, Eugene, OR), the slides were covered, sealed, and stored at 4 °C in the dark until they were observed with a laser-scanning confocal microscope (MRC1024, Bio-Rad, Hercules, CA).

**Confocal Laser Scanning Microscopy Analysis on Live Cells.** WI-L2-729HF2 cells were resuspended in fresh RPMI-1640 supplemented with 10% FCS (growth medium) and counted prior to experimentation. Aliquots of  $4 \times 10^5$  cells in 1 mL of medium were poured into a 6-well plate and allowed to recover for 1 h at 37 °C on an oscillatory shaker. Synthetic peptides, peptides **1a**, **1b**, **2a**, **2b**, **3a**, and **3b**, were then added to a final concentration of 3.0  $\mu$ M, and the incubation was continued for an additional 2 h. The cells were then transferred in Eppendorf tubes and collected by centrifugation (2000 rpm, 2 min), trypsinized with Trypsin-EDTA (Gibco), washed 5 times with growth medium, washed once with PBS, resuspended in 10  $\mu$ L of glycerol-free antifade reagent (50% diluted component B, SlowFade Antifade Kit, Molecular Probes), poured upon a microscope slide, and covered. The excess liquid was aspirated and the

cover slip sealed. The slides were immediately observed with a laser scanning confocal microscope (MRC1024, Bio-Rad) through the DIC (differential interference contrast) and the fluorescence channel. Quantitation of cell-associated fluorescence was determined as follows. A group of an average of 50 cells per experiment (8 bit image) was randomly selected, and the average mean fluorescence intensity over the entire cell area was determined. The error bars are standard deviation calculated for the different values of fluorescence found in each cell. This quantitative image analysis was performed using both BioRad Laser Sharp software and Image J [version 1.32] (NIH image software) and then imported into Excel for further quantitation.

## Results and Discussion

Biochemical mutational analysis of our original RDL-WEMMMVSLACQY-phage (pep1-phage) construct revealed the almost absolute conservation of three contiguous methionine residues (Met 6–8) within the sequence.<sup>22</sup> Interestingly, several groups have reported critical roles of methionine in the pathogenesis of neurodegenerative disorders including Alzheimer's disease and prion-related diseases.<sup>24–27</sup> For example, it has been shown that when the Met-35 residue of  $\beta$ -amyloid is oxidized, the peptide is unable to penetrate lipid membrane and  $\beta$ -sheet formation is inhibited.<sup>26</sup> In light of such precedent, as well as the known biological roles of methionine in protection from oxidative stress,<sup>24,27,28</sup> we investigated the function of the Met(6–8) residues in the interaction of both synthetic monomeric and dimeric forms of peptide **1** with the WI-L2-729HF2 cell membrane as a requisite domain for membrane translocation.

To facilitate the analysis, fluorescein-labeled methionine-modified analogues of peptide **1** (Figure 1) were prepared



**Figure 1.** Primary structure of peptide **1**.

by chemical synthesis in monomeric and symmetrical disulfide-linked dimeric formats using a combination of solid and solution-phase peptide synthesis protocols. All synthetic constructs were prepared with an additional lysine residue at the C-terminus, which was functionalized at the side chain with fluorescein isothiocyanate, isomer 1 (FITC), via an  $\epsilon$ -aminohexanoic acid spacer. Both monomeric and dimeric forms were prepared incorporating reduced Met(6–8) residues (**1a** and **1b**), oxidized Met(6–8) residues (**2a** and **2b**), and norleucine(6–8) (Nle(6–8)) residues (**3a** and **3b**) (Figure 2).

As a confirmation of the results previously obtained with biotin-labeled peptides, the monomer **1a** and dimer **1b** were incubated in the presence of WI-L2-729HF2 cells with and without pretreatment with  $\text{NaN}_3$ .<sup>22,29,30</sup> As expected, internalization of the monomer was not affected by pretreatment of the target cells with  $\text{NaN}_3$  (Figure 3), suggesting that internalization of the monomeric form of this peptide is energy-independent. In contrast, the dimer **1b** exhibited internalization only without  $\text{NaN}_3$  pretreatment (Figure 4), lending further credence to an energy-dependent importation mechanism for this peptide.

To further study the importance of the three contiguous Met(6–8) residues, monomeric and dimeric forms of peptide **1** were prepared using both the sulfoxide (Met-O) forms of methionine (**2a** and **2b**) and the isosteric analogue norleucine (Nle) (**3a** and **3b**). The results of confocal fluorescence microscopy analysis of these analogues are shown in Figures 3 and 4. Internalization of the Met-O(6–8) analogues **2a** and **2b** was negligible regardless of the availability of ATP in the target cells. In contrast, the unoxidizable Nle(6–8) mutants, where the sulfur atom of methionine is replaced by a methylene group, were unable to internalize in the dimeric form **3b**, but behaved similarly to the native sequence in the monomeric form **3a**. These findings as detailed in Figure 5 provide evidence of a cellular uptake mechanism for peptides **1a**, **1b**, and norleucine monomer **3a**; from this figure showing a series of fixed cells, we note that peptides **1b** and **3a** appear to localize in the cytoplasm, whereas **1a** can be found both in cytoplasm and the nucleus.

The uptake of these peptides by the target WI-L2-729HF2 cells was also visualized by differential interference contrast (DIC) microscopy (Figure 6).<sup>31</sup> In this set of experiments the cells were neither fixed nor permeabilized; the results

- (24) Butterfield, D. A.; Kanski, J. Methionine residue 35 is critical for the oxidative stress and neurotoxic properties of Alzheimer's amyloid beta-peptide 1-42. *Peptides* **2002**, *23* (7), 1299–1309.
- (25) Barnham, K. J.; Ciccotosto, G. D.; Tickler, A. K.; Ali, F. E.; Smith, D. G.; Williamson, N. A.; Lam, Y. H.; Carrington, D.; Tew, D.; Kocak, G.; Volitakis, I.; Separovic, F.; Barrow, C. J.; Wade, J. D.; Masters, C. L.; Cherny, R. A.; Curtain, C. C.; Bush, A. I.; Cappai, R. Methionine oxidation and the toxic principle of the beta-amyloid peptide from Alzheimer's disease. *J. Neurochem.* **2003**, *87*, 99–99.
- (26) Barnham, K. J.; Ciccotosto, G. D.; Tickler, A. K.; Ali, F. E.; Smith, D. G.; Williamson, N. A.; Lam, Y. H.; Carrington, D.; Tew, D.; Kocak, G.; Volitakis, I.; Separovic, F.; Barrow, C. J.; Wade, J. D.; Masters, C. L.; Cherny, R. A.; Curtain, C. C.; Bush, A. I.; Cappai, R. Neurotoxic, redox-competent Alzheimer's beta-amyloid is released from lipid membrane by methionine oxidation. *J. Biol. Chem.* **2003**, *278* (44), 42959–42965.
- (27) Butterfield, D. A.; Boyd-Kimball, D. The critical role of methionine 35 in Alzheimer's amyloid-beta-peptide (1-42)-induced oxidative stress and neurotoxicity. *BBA—Proteins Proteomics* **2005**, *1703* (2), 149–156.
- (28) Varadarajan, S.; Yatin, S.; Kanski, J.; Jahanshahi, F.; Butterfield, D. A. Methionine residue 35 is important in amyloid beta-peptide-associated free radical oxidative stress. *Brain Res. Bull.* **1999**, *50* (2), 133–141.
- (29) Wilson, D. F.; Chance, B. Azide Inhibition of Mitochondrial Electron Transport. I. Aerobic Steady State of Succinate Oxidation. *Biochim. Biophys. Acta* **1967**, *131* (3), 421–430.
- (30) Sandvig, K.; Olsnes, S. Entry of the Toxic Proteins Abrin, Modeccin, Ricin, and Diphtheria-Toxin into Cells.2. Effect of Ph, Metabolic-Inhibitors, and Ionophores and Evidence for Toxin Penetration from Endocytotic Vesicles. *J. Biol. Chem.* **1982**, *257* (13), 7504–7513.

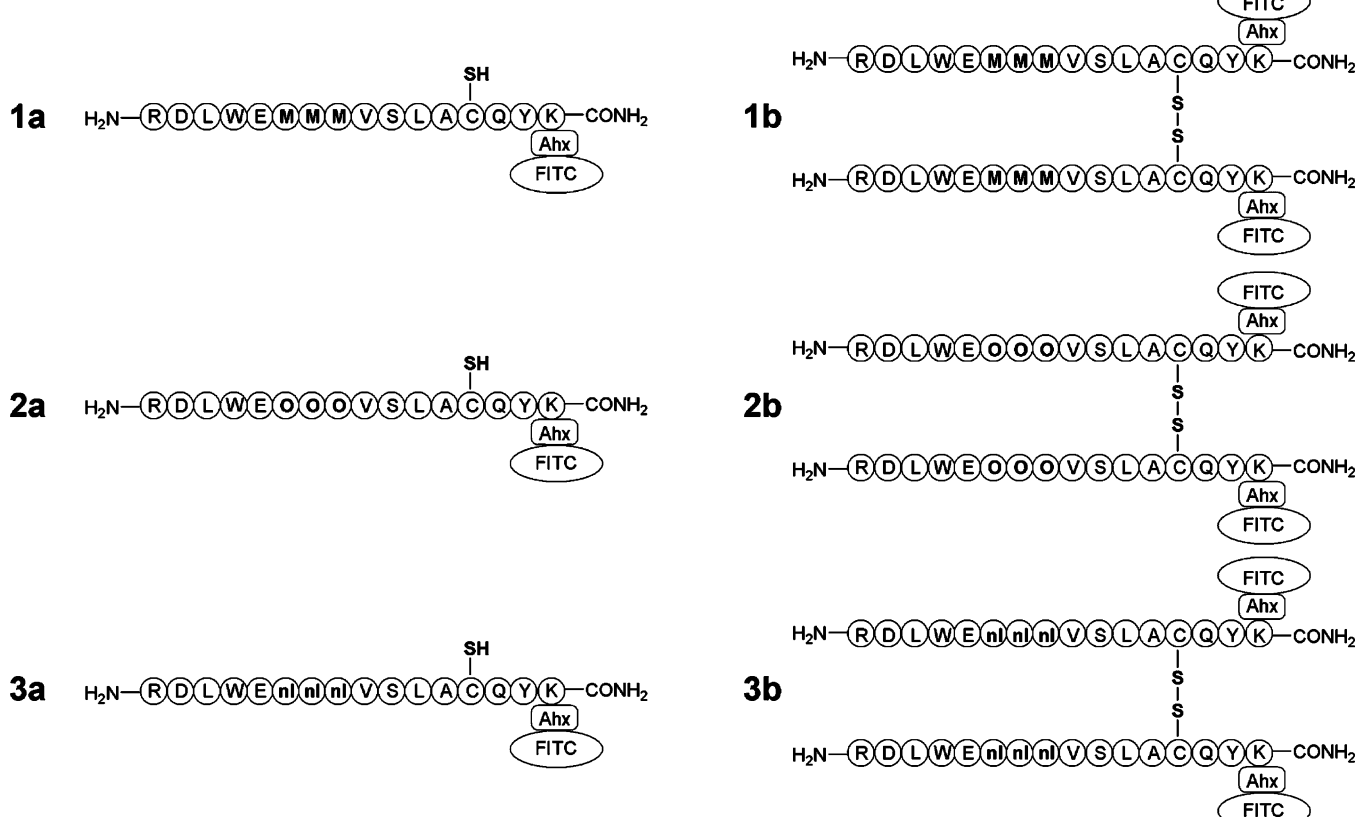


**Figure 2.** Synthetic analogues of peptide 1: monomers **1a**, **2a**, and **3a** and symmetrical dimers **1b**, **2b**, and **3b**. O = methionine sulfoxide, nl = norleucine, and Ahx =  $\epsilon$ -aminohexanoic acid.

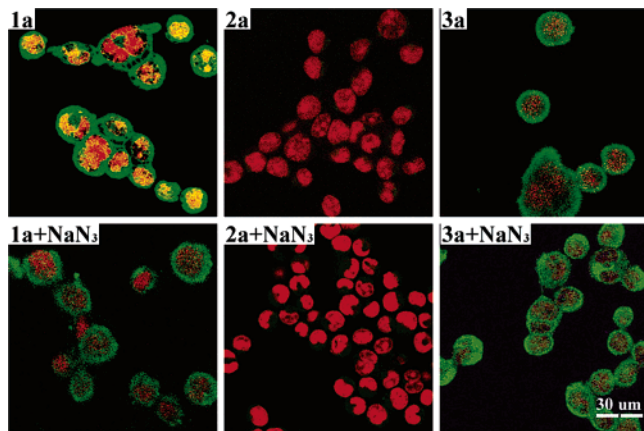


**Figure 3.** Microscopy analysis of FITC-labeled monomeric peptides in the target cells. Green indicates the fluorescence of the FITC-labeled peptide, while red indicates WI-L2-729HF2 cells stained with propidium iodide.

of this visualization method corroborate that peptides **1a**, **1b**, and **3a** are readily internalized and that the outcome of those experiments was not due to an artifact derived from slide preparation. Furthermore, quantification of the fluorescence detected in the live cells visualized by DIC (Figure 7)

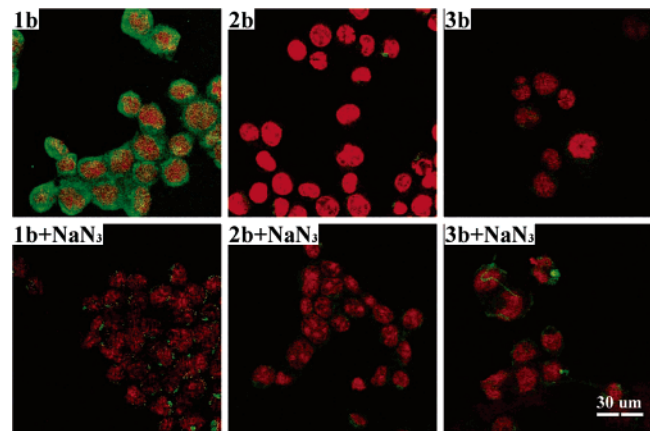


**Figure 4.** Microscopy analysis of fluorescence-labeled (FITC) dimeric analogues in the target cells. Green indicates the fluorescence of the FITC-labeled peptide, while red indicates WI-L2-729HF2 cells stained with propidium iodide.

confirmed that dimer **1b** internalized only in the presence of ATP, monomers **1a** and **3a** showed significant membrane translocation even after ATP depletion, and peptides **2a** and **2b** did not internalize regardless of prior ATP depletion.

It has been noted in the literature that fluorescence microscopy measurements on fixed and permeabilized and/or nondigested cells may not be totally reliable.<sup>7</sup> We believe that our fixed versus live cell experiments support our hypothesis that peptides **1a**, **1b**, and **3a** are cell-penetrating

(31) Chawla, J. S.; Amiji, M. M. Cellular uptake and concentrations of tamoxifen upon administration in poly(epsilon-caprolactone) nanoparticles. *AAPS PharmSci* 2003, 5 (1) (doi:10.1208/ps050103).

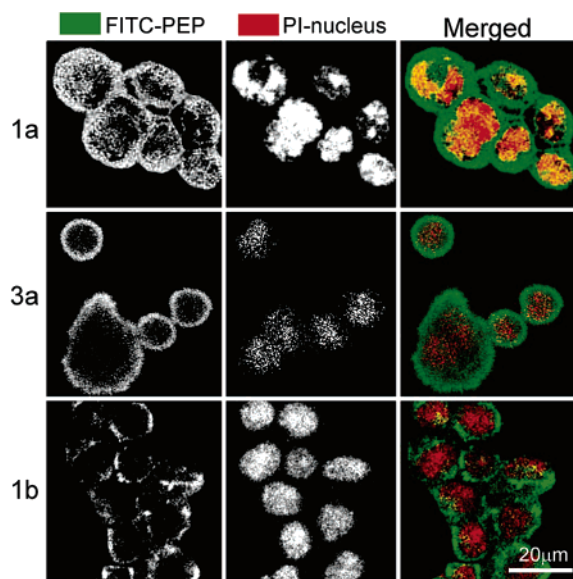


**Figure 5.** Intracellular localization. Microscopy analysis of fluorescence-labeled (FITC) **1a** (wild-type monomer), **3a** (Nle mutant monomer), and **1b** (wild-type dimer) in the target cells. Green indicates the fluorescence of the FITC-labeled peptide, while red indicates WI-L2-729HF2 cells stained with propidium iodide. The colocalization field is shown in the merged image of **1a** as yellow; it describes how the wild-type monomer localizes in both nucleus and cytoplasm while **3a** and **1b** localize only in the cytoplasm of the target cell.

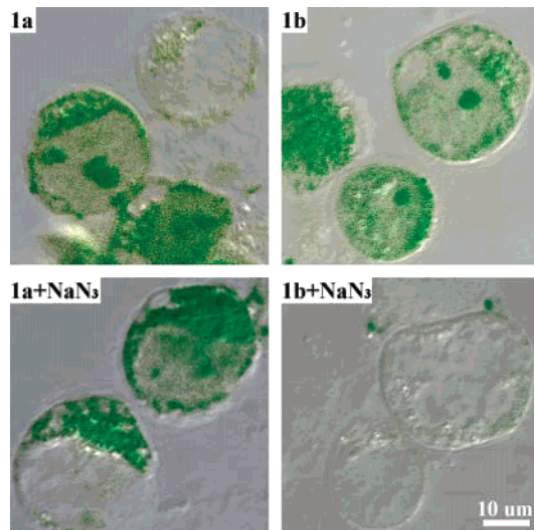


**Figure 6.** Confocal laser scanning microscopy results of the live cells as viewed by DIC (differential interference contrast) microscopy. This slide was prepared by overlaying a fluorescence slide over the DIC picture to demonstrate uptake and localization of peptides. The moon-shaped regions are the living cells, and the green color indicates the FITC-labeled peptide.

peptides. However, these experiments also demonstrate finer details that can be missed using just one of the techniques. Thus, the combination of DIC merged with fluorescence showed an interesting result, wherein the localization of the

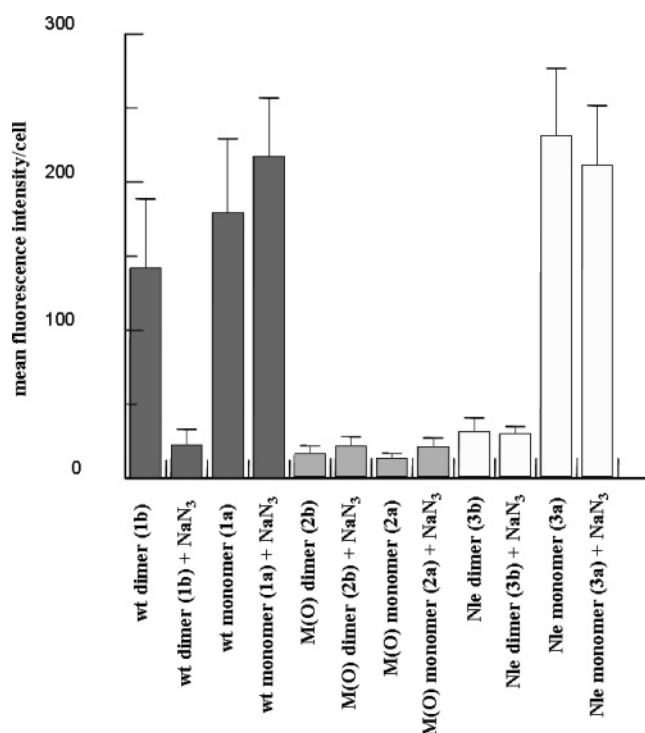


**Figure 7.** Confocal laser scanning microscopy results of the live cells viewed by overlaid DIC (differential interference contrast) and fluorescence images.

wild-type dimer **1b** was also found in the nucleus of the live target cells as a nucleolar accumulation as was the wild-type monomer **1a**. Our hypothesis is that when the dimeric peptide crosses the plasma membrane, the cytoplasmic reducing environment rapidly reduces the disulfide bond of the dimer **1b** to yield two monomers identical to **1a** inside the living cell, and the reduced monomers eventually reach the cell nucleus and remain as nucleolar accumulation.<sup>32–34</sup> Thus, the dissimilar localization outcome of wild-type dimer **1b** between Figures 3–5 and Figure 6 may be a result of the altered cytoplasmic environment inside the plasma membrane. Hence, when the cells are fixed and permeabilized, the altered cytoplasmic environment prevents reduction of the dimer, which results in only the cytoplasmic localization in the fixed cells. However, the overall internalization results which have been detailed, internalization of only **1a**, **1b**, and **3b**, from the fixed cell (Figures 3–5) experiments are confirmed by the live cell experiments with DIC microscope images merged with fluorescence images (Figure 8).

(32) Ziegler, D. M. Role Of Reversible Oxidation-Reduction Of Enzyme Thiols-Disulfides In Metabolic-Regulation. *Annu. Rev. Biochem.* **1985**, 54, 305–329.  
 (33) Hwang, C.; Sinskey, A. J.; Lodish, H. F. Oxidized Redox State Of Glutathione In The Endoplasmic-Reticulum. *Science* **1992**, 257 (5076), 1496–1502.  
 (34) Gilbert, H. F. Molecular And Cellular Aspects Of Thiol Disulfide Exchange. *Adv. Enzymol. Relat. Areas Mol. Biol.* **1990**, 63, 69–172.

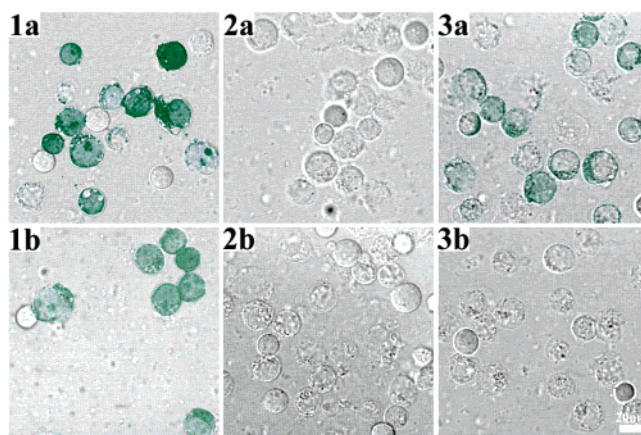


**Figure 8.** Cellular uptake of the peptide analogues in the live cells as viewed by DIC (differential interference contrast) microscopy. This slide was prepared by overlaying a fluorescence slide over the DIC picture to demonstrate uptake and localization of the peptides. The moon-shaped regions are the living cells, and the green color indicates the FITC-labeled peptide.

Such a dimerization-triggered change in membrane translocation to our knowledge has not been previously described for any of the known CPPs. Internalization of the monomer and dimer was abrogated when the peptides were prepared in sulfoxide forms (**2a** and **2b**) prior to their interaction with the cell membrane. Furthermore, in the absence of the native Met thioether side-chain functionality at residues 6–8, monomer **3a** exhibited energy-independent internalization similar to that of the wild-type monomer **1a**, but no internalization was observed with its dimeric congener **3b**. These results suggest that peptide uptake by WI-L2-729HF2 cells mandates a combination of hydrophobic interaction with the cell membrane and an endothermic reaction involving the native Met(6–8) thioether side chains. The substitution of the native Met(6–8) residues with methionine sulfoxide and norleucine therefore impeded internalization by violation of one or both of these mechanistic requirements for the energy-dependent cell-penetrating peptide.

According to our previous findings, there is a high degree of  $\alpha$ -helicity in the structures of **1a** and **1b**, with the monomer **1a** showing 2-fold more intense  $\alpha$ -helicity.<sup>22</sup> However, the effect of the  $\alpha$ -helicity of the monomeric peptide on the energy-independent internalization mechanism remains an open question. To determine whether  $\alpha$ -helicity is a prerequisite for membrane translocation by the monomeric derivatives of this peptide, and whether the solution-phase conformation of the symmetrical dimer differs from that of the monomer, we examined all of the analogues prepared by far-UV circular dichroism under nondenaturing aqueous conditions (Figure 9).

In contrast to the purely  $\alpha$ -helical native monomer and dimer **1a** and **1b**, respectively, the noninternalizing symmetrical Met-O(6–8) dimer **2b** exhibits a combination of  $\alpha$ -helical and  $\beta$ -sheet structure. While this is not rigorously prima facie evidence that uptake of the parent sequence is

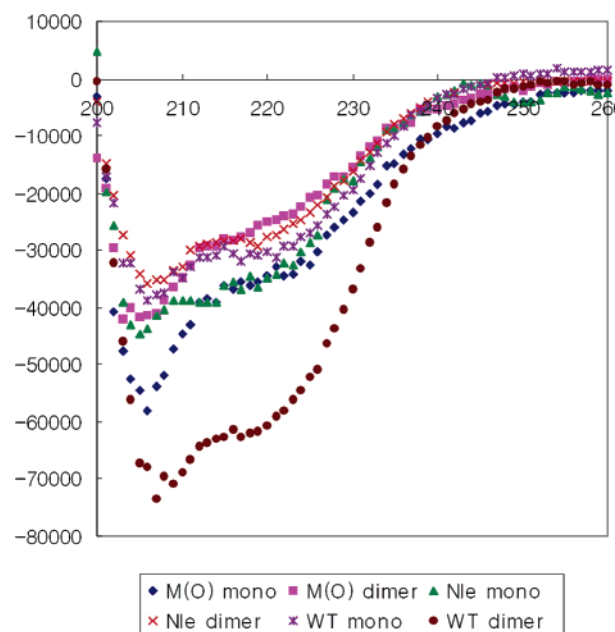


**Figure 9.** Far-UV circular dichroism spectra of peptide analogues.

regulated by a conformational “switch”, such an argument is not unreasonable given the conformational requirements of well-known channel-forming peptides such as gramicidin.<sup>35</sup> Norleucine analogues **3a** and **3b** showed  $\alpha$ -helical CD spectra similar to those of peptides **1a** and **1b**, with negative CD bands at 208 and 220 nm of intensity similar to that of the parent peptides. The high  $\alpha$ -helicity observed for the monomeric Nle(6–8) analogue **3a** correlates well with the nativelike uptake of this analogue by the target cells. This result therefore supports our hypothesis that the passive diffusion of **1a** across the cell membrane of the target WI-L2-729HF2 cells is directly related to its  $\alpha$ -helicity.

## Conclusion

We have demonstrated that, after plasma membrane translocation, the wild-type peptides **1a** and **1b** localize as cytoplasmic and nucleolar accumulation inside the target B-lymphocytes WI-L2-729HF. Furthermore, the uptake of the wild-type symmetrical dimer **1b** is an energy-dependent process that requires the presence of the native Met(6–8) residues, and the same membrane translocation activity of the wild-type monomer **1a** and monomeric Nle(6–8) analogue **3a** indicates that the series of thioether side chains is not a prerequisite for plasma membrane translocation into the target cell in contrast to the dimeric peptide **1b**. Biophysical investigation using far-UV circular dichroism spectroscopy revealed that monomers **1a** and **3a** exhibited approximately 2-fold more intense  $\alpha$ -helicity than dimer **1b**, suggesting that secondary structure might be another key to the monomers’ passive diffusion across the cell membrane.

(35) Wallace, B. A. Recent advances in the high-resolution structures of bacterial channels: Gramicidin A. *J. Struct. Biol.* **1998**, *121* (2), 123–141.

The polarity of the peptide appears critical to both the energy-dependent and energy-independent internalization mechanisms of the wild-type peptides. The hydrophobicity of the midsection of the peptide is probably indispensable to engage an initial interaction with the cell membrane for both monomeric and dimeric peptides. Possible internalization routes via Fenton chemistry and oxidative stress remain for future investigations.

**Acknowledgment.** This work was supported by The Skaggs Institute for Chemical Biology and The National Institutes of Health (CA094193, K.D.J.). We thank Dr. William B. Koisses and the Scripps Core Microscopy Facility for confocal microscopy and differential interference contrast microscopy.

MP050035B